Polymer Journal, Vol. 33, No. 3, pp 227—235 (2001)

Synthesis and Chiroptical Properties of (*S*)-(−)-*N*-α-Methylbenzylmaleimide Polymers Containing Crystallinity

Hua ZHOU, Kenjiro ONIMURA, Hiromori TSUTSUMI, and Tsutomu OISHI†

Department of Applied Chemistry and Chemical Engineering, Faculty of Engineering, Yamaguchi University, 2-16-1 Tokiwadai, Ube, Yamaguchi 755-8611, Japan

(Received August 25, 2000; Accepted December 13, 2000)

ABSTRACT: Chiral (*S*)-(−)-*N*-α-methylbenzylmaleimide ((*S*)-(−)-MBZMI) was polymerized with chiral complexes of (−)-sparteine (Sp) or (*S, S*)-(1-ethylpropylidene)bis(4-benzyl-2-oxazoline) (Bnbox) with organometal in toluene or tetrahydrofuran (THF). Specific rotations $[\alpha]_{435}^{25}$ of the polymers obtained by Et_2Zn/Sp and Et_2Zn/Bnbox were +20.5° to +466.2° and +9.4° to +39.5°, respectively. In the asymmetric anionic polymerization of (*S*)-(−)-MBZMI, Sp was found a more effective chiral ligand than Bnbox. Chirality of the polymers was mainly attributed to different ratios between stereogenic centers (*S, S*) and (*R, R*) in the main chain produced by asymmetric induction. Crystalline poly((*S*)-(−)-MBZMI)s obtained with Et_2Zn/Sp at lower temperatures in toluene having specific rotations $[\alpha]_{435}^{25}$ more than +200° showed higher stereoregularity, compared to that of poly((*R*)-(+)-MBZMI) under the same conditions, judging from X-Ray diffraction diagrams and ^{13}C NMR spectra. Chiroptical properties of these polymers may partially be due to helical conformation.

KEY WORDS Chiral *N*-Substituted Maleimide / Chiral Ligand / Asymmetric Anionic Polymerization / Optically Active Polymer / Crystallinity /

Asymmetric anionic polymerizations of bulky methacrylate, isocyanate and acetylene derivatives with chiral ligand-organometal complexes were systematically carried out by Okamoto *et al.* to give optically active polymers with one handed-helical conformation.[1-3]

Up to now, asymmetric anionic polymerizations of achiral *N*-substituted maleimide (RMI)[4-11] have been studied using chiral ligand-organometal complexes to obtain optically active poly(RMI). More recently, the authors obtained optically active poly(RMI) with higher specific rotations.[5-10] Chirality of the polymers was attributed to excess chiral stereogenic centers (*S, S*) and (*R, R*) in the polymer main chain based on threo-diisotactic structures formed from asymmetric polymerization. Polymerizations and copolymerizations of chiral RMI have been studied by the authors.[12-16] A new chirality was introduced onto the main chain of poly(RMI) in spite of poly(RMI) having small specific rotation. Asymmetric anionic polymerizations of chiral (*R*)-(+)-*N*-α-Methylbenzylmaleimide ((*R*)-(+)-MBZMI)[17] using chiral complexes of Sp or (*S, S*)-(1-ethylpropylidene)-bis(4-benzyl-2-oxazoline) (Bnbox) with organometal were found to afford optically active polymers having higher specific rotations than those of poly((*R*)-(+)-MBZMI) obtained with radical and anionic initiators.[18] However, there have been no investigations on asymmetric anionic polymerizations of chiral (*S*)-(−)-MBZMI.

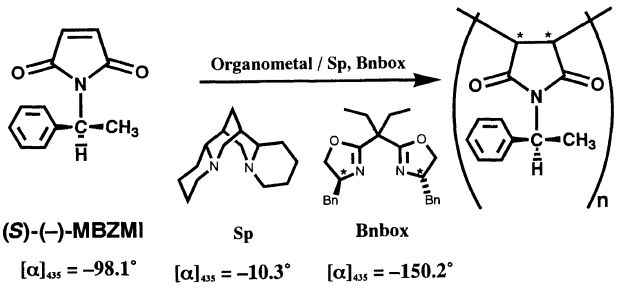

Scheme 1.

This paper describes asymmetric anionic polymerizations of chiral (*S*)-(−)-MBZMI with Et_2Zn/Sp or Et_2Zn/Bnbox complexes as initiator in toluene or tetrahydrofuran (THF), as shown in Scheme 1. Polymers obtained with Et_2Zn/Sp at lower temperatures in toluene had fairly high specific rotation and exhibited higher crystallinity, compared with poly((*R*)-(+)-MBZMI) obtained under the same conditions. The effects of temperature, time and ratio of ligand to organometal on asymmetric anionic polymerization of (*S*)-(−)-MBZMI were investigated in detail. Asymmetric induction to the polymer main chain is discussed by circular dichroism spectra (CD), and GPC analysis with UV and polarimetric detectors. The structure and crystallinity of poly((*S*)-(−)-MBZMI) are discussed based on measurements of ^{13}C NMR spectra and X-Ray diffraction spectra.

EXPERIMENTAL

Materials

(*S*)-(−)-MBZMI was synthesized by reported previously.[19]

(*S*)-(−)-MBZMI: bp 177—178℃ / 6 mmHg; $[\alpha]_{435}^{25} = -98.1°$ ($c = 1.0$ g dL^{-1}, THF, $l = 10$ cm). ^1H NMR spectrum: chemical shift, δ in ppm from $Si(CH_3)_4$ in $CDCl_3$: 7.45—7.15 (m, 5H, phenyl), 6.65 (s, 2H, CH=CH), 5.35 (q, 1H, $J = 7.6$ Hz, CH), 1.85 (d, 3H, $J = 7.6$ Hz, CH_3), ^{13}C NMR: δ in ppm from $Si(CH_3)_4$ in $CDCl_3$: 170.53 (C=O), 140.30, 128.44, 127.62, 127.12 (phenyl), 133.92 (CH=CH), 49.49

†To whom all correspondence should be addressed.

(CH), 17.90 (CH_3).

A model compound, (*S*)-(−)-*N*-α-methylbenzylsuccinimide ((*S*)-(−)-MBZSI): bp 163—165℃ / 5 mmHg; mp 59—61℃; $[\alpha]_{435}^{25} = -142.6°$ ($c = 1.0$ g dL^{-1}, THF, $l = 10$ cm), ^{1}H NMR spectrum: chemical shift, δ in ppm from $Si(CH_3)_4$ in $CDCl_3$: 7.50—7.20 (m, 5H, phenyl), 5.43 (q, 1H, $J = 7.3$ Hz, CH), 2.65 (m, 4H, CH_2–CH_2), 1.85 (d, 3H, $J = 7.3$ Hz, CH_3). ^{13}C NMR: δ in ppm from $Si(CH_3)_4$ in $CDCl_3$: 176.73 (C=O), 139.39, 128.00, 127.33, 127.19 (phenyl), 49.78 (CH), 27.68 (CH_2–CH_2), 16.18 (CH_3).

Solvents in the reaction and polymerization were purified by usual methods.[20] Commercially available *n*-butyllithium (*n*-BuLi) hexane solution (1.53 mol L^{-1}) and diethylzinc hexane solution (1.02 mol L^{-1}) were used without further purification. *n*-BuLi and Et_2Zn were determined from titration using HCl solution. (*S, S*)-(1-Ethylpropylidene)bis(4-benzyl-2-oxazoline) (Bnbox) was prepared as reported previously.[21] ($[\alpha]_{435}^{25} = -150.7°$, $c = 1.0$ g dL^{-1}, THF, $l = 10$ cm). Commercially available (−)-sparteine (Sp) was purified by distillation under reduced pressure: bp 93—94℃ / 5×10^{-2} mmHg; ($[\alpha]_{435}^{25} = -10.3°$ ($c = 1.0$ g dL^{-1}, THF, $l = 10$ cm).

Anionic Polymerizations

(*S*)-(−)-MBZMI was placed in a schlenk reaction tube and toluene or THF was added to dissolve it. This procedure was performed under nitrogen atmosphere. The monomer solution was cooled to polymerization temperature, and catalyst solution was added using a cannula. Polymerization was completed by the addition of methanol solution containing a small amount of hydrochloric acid. Polymerization solution was poured into excess methanol to precipitate the polymers. The polymers were purified three times by precipitation from a small amount of THF solution to excess methanol. The obtained pure polymers were dried *in vacuo* at r.t. for 2 days.

Radical Polymerization

Radical polymerizations were conducted with AIBN as initiator in toluene in a sealed tube at 60℃. After polymerization, the polymer solution was poured into a large amount of methanol to precipitate the polymer. The polymer was purified by reprecipitation twice from THF solution to excess methanol, filtered and dried *in vacuo* at r.t. for 2 days.

Measurements

Specific rotation was measured in THF at 25℃ using a quartz cell (5 and 10 cm) with a JASCO DIP-140 (JASCO Co. Ltd.). CD spectra were measured in THF at 25℃ using a quartz cell of 0.1 mm with a JASCO J20C (JASCO Co. Ltd.). UV spectra were obtained by measurement at 25℃ in THF using a quartz cell of 1 mm. Number-average molecular weights (M_ns) of the polymers were measured by gel permeation chromatography (GPC) using THF as eluant and polystyrene as standard at 50℃ with a Shimadzu LC-10A instrument equipped with a UV-visible photo spectrometer SPD-10A, polarimetric detector (JASCO OR-990) and data processor. ^{1}H and ^{13}C NMR spectra were obtained with a JEOL-EX 270 (Nippon Electric Co., Ltd.). X-Ray diffraction patterns were measured using an X-Ray diffractometer (SHIMADZU XD-D1).

RESULTS AND DISCUSSION

Anionic and Radical Polymerizations of (S)-(−)-MBZMI

Table I shows the results of anionic and radical polymerizations of (*S*)-(−)-MBZMI initiated by *n*-BuLi and Et_2Zn in toluene or THF. Specific rotations of the polymers were influenced by different organometal initiators. The polymers obtained with *n*-BuLi exhibited levo optical rotation. Using Et_2Zn as initiator, the polymers showed dextro specific rotation except for run 3 in Table I. The polymer obtained with Et_2Zn in toluene at r.t. showed higher absolute specific rotation than that at 0℃. In THF, the polymer initiated by Et_2Zn exhibited higher specific rotation at 0℃ than that at r.t.

Racemization of optically active moiety in chiral (*S*)-(−)-MBZMI hardly occurred in the polymerization with BuLi under the above conditions due to the mechanism of anionic polymerization. Butyl anions preferentialy attack carbons on double bonds by nucleophilic reaction because Li cation coordinates with oxygen of the carbonyl group resulting in transfer of electrons of carbon on double bonds. Specific rotations of poly((*S*)-(−)-(MBZMI) obtained with BuLi support these results. In the polymerization of (*S*)-(−)-methylbenzylmethacrylate ((*S*)-(−)-MBMA) with BuLi under the same conditions as for (*S*)-(−)-MBZMI, no racemization of (*S*)-(−)-MBMA took place.[22,23] When (*RS*)-(±)-MBMA) was enantiomerically polymerized, the optically active monomer was recovered and no racemization of chiral MBMA was observed.[24,25]

Specific rotations of the polymers formed by the same organometal initiators were influenced by different solvents. The polymers obtained with Et_2Zn in THF showed larger dextro specific rotation, yield and M_n than those with the same initiator in toluene. Poly((*S*)-(−)-MBZMI)

Table I. Anionic or radical polymerizations of (*S*)-(−)-MBZMI[a]

Run	Initiator	Polym. solvent	Polym. temp.	Polym. time	Yield[b]	M_n[c] $\times 10^{-3}$	M_w/M_n[c]	$[\alpha]_{435}^{25}$[d]
	mol%	mL	℃	h	%			deg.
1	*n*-BuLi(10)	Tol.(5)	0	24	58.9	3.1	1.6	−94.5
2	*n*-BuLi(10)	THF(5)	0	24	38.9	5.2	1.3	−7.8
3	Et_2Zn(10)	Tol.(5)	r.t.	120	61.4	3.1	1.4	−106.9
4	Et_2Zn(10)	THF(5)	r.t.	120	76.4	17.9	1.3	+66.6
5	Et_2Zn(10)	Tol.(5)	0	120	52.8	9.1	6.2	−22.0
6	Et_2Zn(10)	THF(5)	0	120	74.5	4.5	2.2	+74.5
7	AIBN(5)	Tol.(5)	60	24	88.1	3.0	1.9	−30.1

[a] [Monomer] = 0.5 mol L^{-1}. [b] MeOH-insoluble. [c] By GPC. [d] $c = 1.0$ g dL^{-1}, $l = 10$ cm, THF.

obtained with Et_2Zn in toluene at 0℃ had poor yield, M_n and lower specific rotation.

The polymer obtained with AIBN showed specific rotation −30.1° (Run 7 in Table I) and M_n of 3.0×10^3, which were similar to those reported previously.[18]

Specific rotations ($[\alpha]^{25}_{435}$ −94.5°—+1.5°) of the polymers obtained by only an organometal initiator were quite different from those of the starting monomer (*S*)-(−)-MBZMI ($[\alpha]^{25}_{435}$ −98.1°) and model compound (*S*)-(−)-MBZSI ($[\alpha]^{25}_{435}$ −142.6°), suggesting a new chirality of the polymer may be introduced onto the polymer main chain by optically active groups of (*S*)-(−)-MBZMI during polymerization. These results were similar to those reported proviously.[17]

Asymmetric Anionic Polymerization of (S)-(−)-MBZMI

Tables II and III show the results of asymmetric anionic polymerizations of chiral (*S*)-(−)-MBZMI with Sp / organometal complexes in toluene or THF at different temperatures. Poly((*S*)-(−)-MBZMI) formed by *n*-BuLi/Sp exhibited levo specific rotations ($[\alpha]^{25}_{435}$ −17.7°—−77.8°). M_ns of the polymers were between 2.6×10^3 and 8.2×10^3. Yields and M_ns of the polymers obtained with *n*-BuLi/Sp in THF were higher than those in toluene.

Specific rotations ($[\alpha]^{25}_{435}$) of the polymers prepared by Et_2Zn/Sp were +20.5° to +466.2°, opposite those of polymers obtained with *n*-BuLi/Sp. The same was observed in the polymerization of (*R*)-(+)-MBZMI reported previously.[17] Crystalline poly((*S*)-(−)-MBZMI)s having higher specific rotation ($[\alpha]^{25}_{435}$: +242.2° to +466.2°) were synthesized with the E_2Zn/Sp complex in toluene at 0℃ and −35℃. In these cases, polymerizations proceeded in a heterogeneous system during polymerization, which results from low solubility of (*S*)-(−)-MBZMI monomer in toluene at low temperatures. The poly((*S*)-(−)-MBZMI)s were partly insoluble in toluene. Yields and specific rotations of the polymers obtained by Sp increased by long reaction periods. The reason may be as follows. The poly((*S*)-(−)-MBZMI) growth-end very slowly and selectively attacks a monomer at lower temperatures. Since the obtained poly((*S*)-(−)-MBZMI) was not soluble in organic solvents such as THF and DMF, M_n could not be measured by GPC. Polymerization time exceeded 120 h, and specific rotations of the polymers THF-insoluble remarkably increased. Poly((*S*)-(−)-MBZMI) obtained at −35℃ for 144 h exhibited the highest positive specific rotation of +466.2° (Run 4 in Table III). THF-insoluble parts of the polymer showed specific rotation ($[\alpha]^{25}_{435}$)=+551.7° in $CHCl_3$, Run 4 in Table III). The specific rotation of THF-insoluble parts of the polymer increased with polymerization time, but the yields decreased. These specific rotations of polymers were quite different from those of optically active monomer (*S*)-(−)-MBZMI ($[\alpha]^{25}_{435}$=−98.1°), model compound (*S*)-(−)-MBZSI ($[\alpha]^{25}_{435}$=−142.6°) and poly((*S*)-(−)-MBZMI) ($[\alpha]^{25}_{435}$=−106.9° to +74.5°) obtained with only Et_2Zn. Chirality of the polymers may be introduced into polymer main chain by asymmetric induction by chiral ligand-organometal complexes. However, no polymerizations of (*S*)-(−)-MBZMI initiated by Et_2Zn/Sp proceeded in toluene at −78℃.

Using low basic organometals such as Et_2Zn, specific rotations of the polymers were efficiently influenced by different ligands. Table IV shows the results of asymmetric anionic polymerizations of (*S*)-(−)-MBZMI with Et_2Zn/Bnbox complex in toluene or THF. All polymers showed dextro specific rotations (+9.4°—+39.5°) and higher M_n (8.9×10^3—2.7×10^4). At r.t., the polymers obtained in THF showed the highest specific rotation (+39.5°) and higher M_n (2.7×10^4; Run 4 in Table IV), possibly due to less bulkiness of Bnbox than Sp.[6] That is, the Et_2Zn/Sp complex builds better asymmetric fields at poly((*S*)-(−)-MBZMI) growth-end than Et_2Zn/Bnbox. Chirality of the polymers prepared with Et_2Zn/Sp may

Table II. Asymmetric anionic polymerizations of (*S*)-(−)-MBZMI[a] with sparteine

Run	Initiator[a] mol%	Polym. solvent mL	Polym. temp. ℃	Polym. time h	Yield[c] %	M_n[d]$\times10^{-3}$	M_w/M_n[d]	$[\alpha]^{25}_{435}$[e] deg.
1	Et_2Zn/Sp(10)	Tol.(5)	0	72	100	74.8[f]	10.0	+242.2[g](206.0[f])
2	Et_2Zn/Sp(10)	THF(5)	0	72	100	16.7	2.8	+84.8
3	Et_2Zn/Sp(10)	Tol.(5)	r.t.	72	89.2	8.9	3.2	+20.5
4	Et_2Zn/Sp(10)	THF(5)	r.t.	72	95.6	11.4	2.2	+33.8
5	*n*-BuLi/Sp(10)	Tol.(5)	0	24	78.0	2.6	1.6	−57.5
6	*n*-BuLi/Sp(10)	THF(5)	0	24	83.4	8.2	1.9	−17.7
7	*n*-BuLi/Sp(10)	Tol.(5)	r.t.	24	82.3	3.2	1.9	−70.0
8	*n*-BuLi/Sp(10)	THF(5)	r.t.	24	54.8	2.8	1.5	−77.8

[a] [Monomer]=0.5 mol L^{-1}. [b] [Et_2Zn]/[Ligand]=1.0/1.2. [c] MeOH-insoluble part. [d] By GPC. [e] c=1.0 g dL^{-1}, l=10 cm, THF. [f] THF-soluble. [g] c=1.0 g dL^{-1}, l=10 cm, $CHCl_3$.

Table III. Asymmetric anionic polymerizations of (*S*)-(−)-MBZMI with sparteine[a] for −35℃

Run	Polym. time h	Polym. Yield[c] %	M_n[d]$\times10^{-3}$	M_w/M_n[d]	$[\alpha]^{25}_{435}$[f] deg.	THF-soluble Yield %	THF-soluble $[\alpha]^{25}_{435}$[e] deg.	THF-insoluble Yield %	THF-insoluble $[\alpha]^{25}_{435}$[f] deg.
1	72	14.8	10.5	13.4	+346.9				
2	98	19.1	—	—	+409.4				
3	120	79.5	—	—	+410.6	76.5	+145.1	23.5	+488.4
4	144	80.5	—	—	+466.2	81.1	+111.9	18.9	+551.7

[a] [Monomer]=0.5 mol L^{-1}, in toluene. [b] [Et_2Zn]/[Ligand]=1.0/1.2. [c] MeOH-insoluble part. [d] By GPC. [e] c=1.0 g dL^{-1}, l=10 cm, THF. [f] c=1.0 g dL^{-1}, l=10 cm, $CHCl_3$.

Table IV. Anionic polymerizations of (*S*)-(−)-MBZMI with Bnbox[a]

Run	Initiator[b]	Polym. solvent	Polym. temp.	Polym. time	Yield[c]	M_n[d]$\times 10^{-3}$	M_w/M_n[d]	$[\alpha]_{435}^{25}$[e]
	mol%	mL	℃	h	%			deg.
1	Et_2Zn/Bbox(10)	Tol.(5)	0	72	99.6	13.2	2.1	+9.4
2	Et_2Zn/Bnbox(10)	THF(5)	0	72	100	8.9	2.4	+36.1
3	Et_2Zn/Bnbox(10)	Tol.(5)	r.t.	72	100	10.9	2.9	+36.5
4	Et_2Zn/Bnbox(10)	THF(5)	r.t.	72	100	27.2	2.5	+39.5

[a] [Monomer] = 0.5 mol L^{-1}. [b] [Et_2Zn]/[Ligand] = 1.0/1.2. [c] MeOH-insoluble part. [d] By GPC. [e] c = 1.0 g dL^{-1}, l = 10 cm, THF.

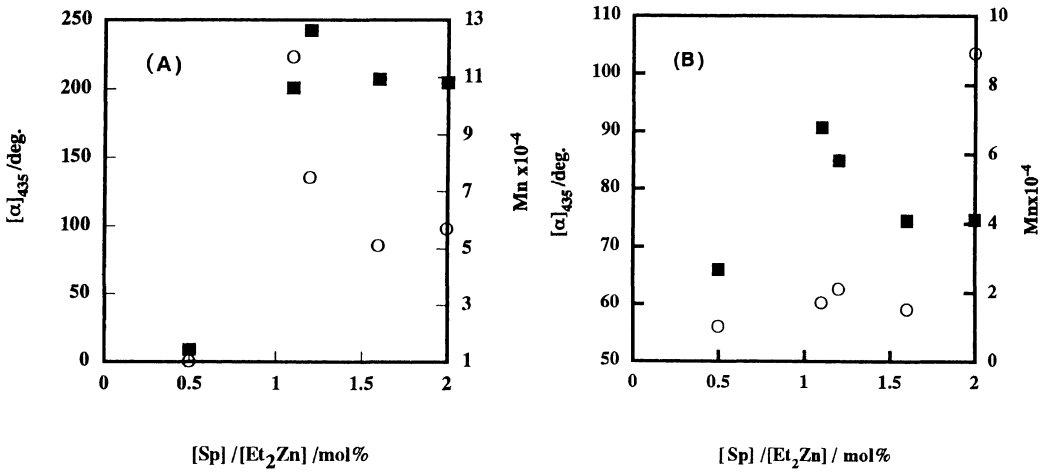

Figure 1. Effects of [Sp]/[Et_2Zn] on specific rotations (■) and M_n (○) of poly((*S*)-(−)-MBZMI) obtained with Et_2Zn/Sp in (A) toluene and (B) THF at 0℃.

be greatly introduced into main chain of poly((*S*)-(−)-MBZMI), compared with Et_2Zn/Bnbox.

The effects of molar ratios of Sp and Et_2Zn on the specific rotations and M_ns of poly((*S*)-(−)-MBZMI) obtained in toluene or THF at 0℃ are summaried in Figure 1. Using toluene (A in Figure 1), the specific rotation was greatest when the molar ratio of Sp and Et_2Zn was 1.2/1.0. M_n was largest when the molar ratio of Sp and Et_2Zn was 1.0/1.0. Polymerizability of (*S*)-(−)-MBZMI initiated by the Et_2Zn/Sp complex was higher than that by only Et_2Zn, as shown in Tables I and II. Polymerizations were carried out by the molar ratio of Sp and Et_2Zn in 0.5/1.0 to give poly((*S*)-(−)-MBZMI) having lower specific rotation. By excess Sp, the polymer obtained with the molar ratio of Sp and Et_2Zn in the range of 1.6/1.0 to 2.0/1.0 exhibited lower specific rotations. In these cases, Et_2Zn/Sp complexes were considered difficult to build better asymmetric fields at the polymer growth-end. In case of THF, when the ratio of Sp and Et_2Zn was 1.2/1.0, the polymer showed the highest specific rotation. But the polymer exhibited the highest M_n when the molar ratio of Sp and Et_2Zn was 1.0/2.0. The reason for this is not clear at present.

To observe directly changes in optical rotation in toluene or THF during asymmetric anionic polymerizations of (*S*)-(−)-MBZMI, polymerizations of (*S*)-(−)-MBZMI were carried out with Et_2Zn/Sp in a 1.0 cm quartz cell in toluene or THF at 25℃. Figure 2 shows changes of optical rotation in toluene (or THF) during polymerization at [initiator]/[(*S*)-(−)-MBZMI] = 10%, [Et_2Zn]/Sp = 1.0/1.2, and 0.5 mol L^{-1}. Using toluene as solvent, the initial optical rotation of only monomer (*S*)-(−)-MBZMI was −1.14° ($[\alpha]_{435}^{25}$) at then decreased in a positive direction as polymerization proceeded. Optical rotation of the solution became positive after 35 min. It was difficult to measure optical rotation of the solution after 50 min because of dark red color of the polymerization solution. For THF, the same was observed. But the initial optical rotation of only monomer (*S*)-(−)-MBZMI was −0.95°. Optical rotation of the solution became positive after *ca.* 15 min from the start of polymerization, and the optical rotation reached a constant value ($[\alpha]_{435}^{25}$ +0.25°) after *ca.* 25 min from the initiation polymerization. The rate

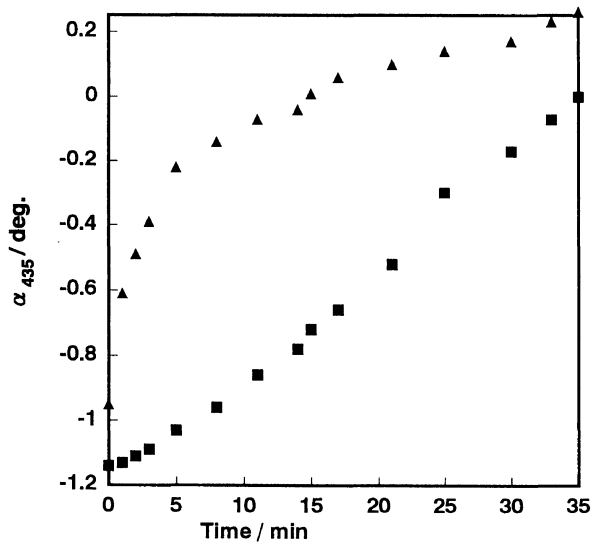

Figure 2. Change in optical rotations for polymerization systems of (*S*)-(−)-MBZMI with Et_2Zn/Sp in toluene (■) and THF (▲) at 25℃ in a quartz cell.

of polymerization of (*S*)-(−)-MBZMI in THF is thus larger than in toluene.

Figure 3 shows the effects of polymerization temperatures on specific rotation and M_n of poly((*S*)-(−)-MBZMI) obtained by Et_2Zn/Sp in toluene or THF. The polymer obtained in toluene at −35℃ for 72 h showed the highest positive specific rotation ($[\alpha]^{25}_{435}=+346.9^\circ$), but M_n was highest at 0℃. In THF, the polymer obtained at 0℃ showed higher specific rotation and M_n ($[\alpha]^{25}_{435}=+84.8^\circ$; $M_n=1.7\times10^4$). The obtained polymers at r.t. showed lower specific rotation and poor M_n, suggesting polymerization temperature to be essential for the asymmetric anionic polymerization. These results can be explained by the same reason as for polymerization of (*R*)-(+)-MBZMI.[17]

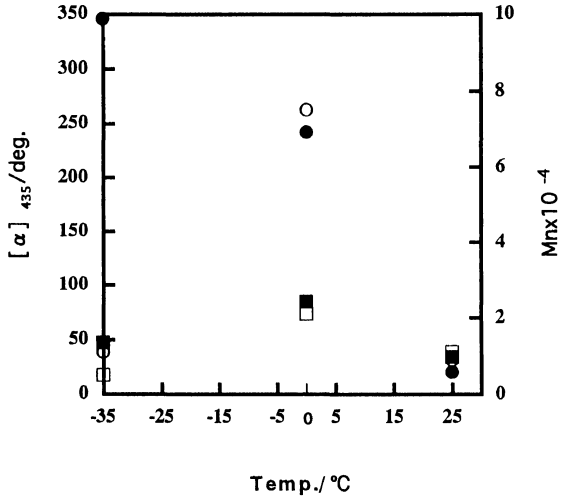

Figure 3. Effects of polymerization temperatures on specific rotation (■, ●) and M_n(□, ○) of poly((*S*)-(−)-MBZMI) obtained with Et_2Zn/Sp in solvents: THF: ■, □; toluene: ●, ○.

CD and UV spectra for the polymers, model compound and monomer are shown in Figure 4. Negative and positive peaks of the poly((*S*)-(−)-MBZMI) formed by *n*-BuLi (1), Et_2Zn/Sp (2) (3), AIBN (4) appeared at 230 nm and 255 nm, respectively, due to $n \rightarrow \pi^*$electric transition of carbonyl groups in the maleimide ring and $\pi \rightarrow \pi^*$ electric transition of phenyl groups in (*S*)-(−)-MBZMI units of the polymer main chain. Positive CD peaks of the poly((*S*)-(−)-MBZMI)s obtained by Et_2Zn/Sp, *n*-BuLi and AIBN at 255 nm have mirror images to those of poly((*R*)-(+)-MBZMI)[17] obtained under the same conditions, which were different from that of model compound poly((*S*)-(−)-MBZSI) (5), but similar to that of monomer (*S*)-(−)-MBZMI (6). It is clear that the chirality of obtained polymers depends on that of chiral MBZMI. In other words, opposite chirality of poly((*S*)-(−)-MBZMI) to poly((*R*)-(+)-MBZMI) may be due not only to asymmetric induction by chiral ligand-organometal complexes but also to chiral α-methylbenzyl group of (*S*)-(−)-MBZMI. Optically active ligand may significantly influence chirality of poly((*S*)-(−)-MBZMI), because the poly((*S*)-(−)-MBZMI)s obtained with Sp/Et_2Zn showed sharper peaks in the ^{13}C NMR and ^1H NMR, and higher crystalline, judging by XRD. CD spectral patterns of poly((*S*)-(−)-MBZMI)s obtained by BuLi, AIBN and chiral ligand-organometal complexes were similar. These polymers may thus have similar structures.[17] In the polymerization with Et_2Zn/Sp ((2), (3), in Figure 4), the larger the positive specific rotation, the higher the peak at 255 nm appeared (positive "Cotton Effect"), suggesting asymmetric induction to more effectively take place in polymer main chains.

Figure 5 shows GPC curves of (+)-poly((*S*)-(−)-MBZMI) (Run 1 in Table II) and (+)-poly((*S*)-(−)-MBZMI) (Run 1 in Table IV) by GPC equipped with UV

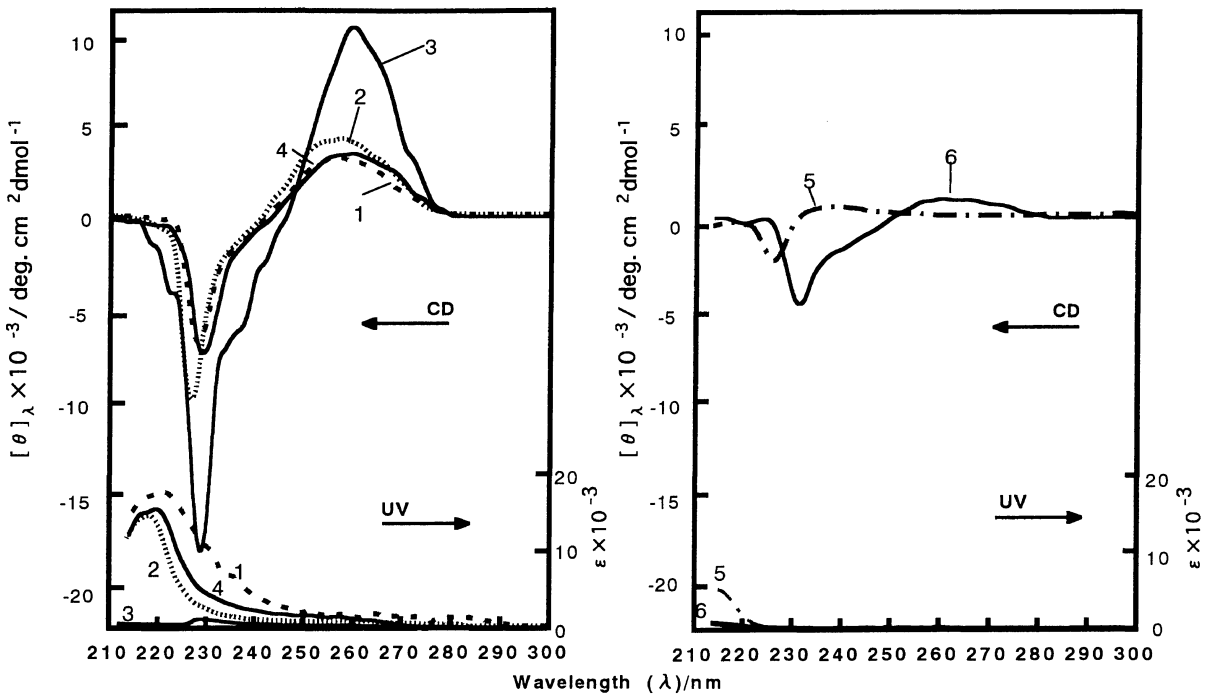

Figure 4. CD and UV spectra for poly((*S*)-(−)-MBZMI) obtained with (1) *n*-BuLi (Run 2 in Table I), (2) Et_2Zn/Sp (Run 1 in Table II), (3) Et_2Zn/Sp (Run 4 in Table III), (4) AIBN (Run 6 in Table I), (5) (*S*)-(−)-MBZSI, and (6) (4) (*S*)-(−)-MBZMI.

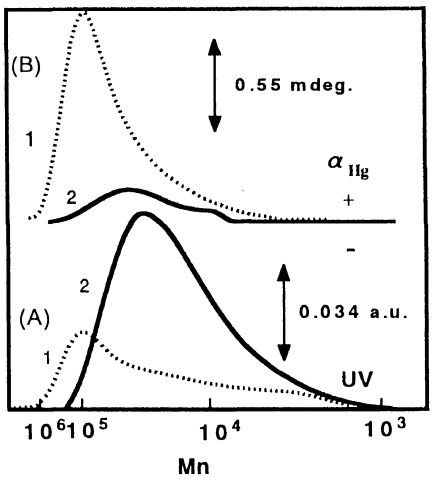

Figure 5. GPC curves of poly((*S*)-(−)-MBZMI) prepared with (1) Et_2Zn/Sp (run 1 in Table II), (2) Et_2Zn/Bnbox (run 1 in Table IV). Top chromatogram was obtained by (A) polarimetric detection (α_{Hg}) and the one on bottom by (B) UV detector.

(1) and polarimetric detector (2). In the GPC curves of poly((*S*)-(−)-MBZMI) prepared with Et_2Zn/Sp by a UV detector (A-1), the polymer included only one high molecular weight fraction and the peak appeared in the same region as that by polarimetric detector (B-1), which suggests that whole polymer main chains are optically active. GPC curves (A-2, B-2) of the poly((*S*)-(−)-MBZMI) obtained by Et_2Zn/Bnbox exhibited similar peaks, compared with those obtained with Et_2Zn/Sp. The whole polymer main chain was optically active, and the curve (B-2) by polarimetric detector also indicated a positive sign in the whole region. But M_n of the polymer obtained with Et_2Zn/Sp was higher than that of the polymer obtained with Et_2Zn/Bnbox. Intensity of the positive peak by a curve (B-1) was larger than that by a curve (B-2), which was in an agreement with the magnitude and sign of the specific rotation of polymer. Sp influenced the stereoregularity of the polymer main chain more than Bnbox. This was supported by the fact that the specific rotation of the polymer obtained with Et_2Zn/Sp was larger than that of the polymer with Et_2Zn/Bnbox although absolute specific rotation of Bnbox was larger than that of Sp.

Polymer Structures

^1H NMR spectra for the polymers obtained with Et_2Zn/Sp, BuLi and AIBN were different, as shown in Figure 6. The different peaks at 3—4 ppm assigned to methine protons (a) of the main chain suggest that polymer main chains may contain different configuration units after trans-opening of double bonds.

Expanded ^{13}C NMR spectra for poly((*S*)-(−)-MBZMI) obtained with Et_2Zn/Sp (1), *n*-BuLi (2), and AIBN (3) are shown in Figure 7. Peaks at 43 ppm were assigned to main chain carbons of poly((*S*)-(−)-MBZMI). Peaks at about 17 and 176 ppm were due to methyl carbons and carbonyl carbons, respectively. Peaks for poly((*S*)-(−)-MBZMI) formed by BuLi (2) and AIBN (3) were different from those with Et_2Zn/Sp (1). All poly((*S*)-(−)-MBZMI) obtained with Et_2Zn/Sp showed sharper peaks than those with other initiators under the same conditions.

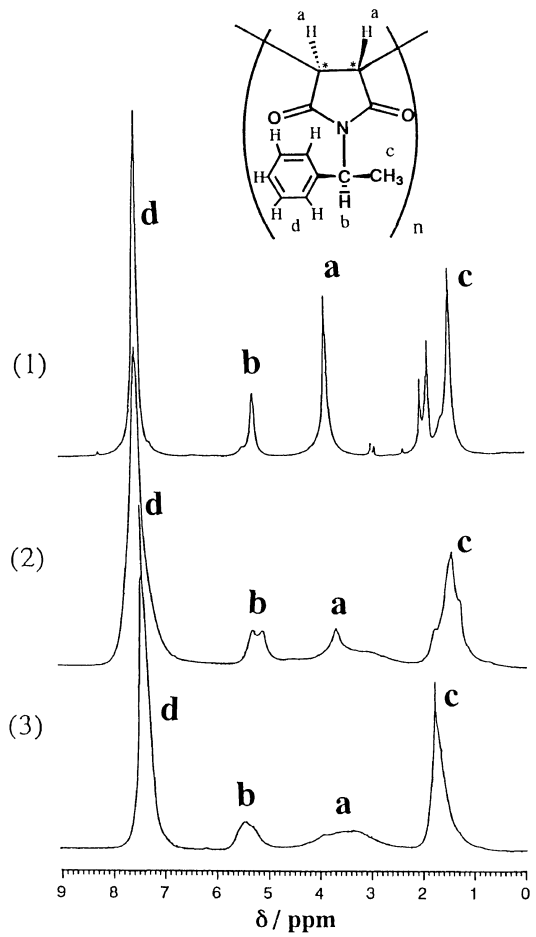

Figure 6. ^1H NMR spectra for poly((*S*)-(−)-MBZMI) obtained with (1) Et_2Zn/Sp: $[\alpha]_{435}$ +551.7°, (2) *n*-BuLi: $[\alpha]_{435}$ −7.8°, and (3) AIBN: $[\alpha]_{435}$ −30.1°.

Asymmetric induction may thus take place in the polymer main chain and polymers obtained with Et_2Zn/Sp (1) may show higher stereoregularity than that obtained with other anionic (2) and radical (3) initiators. But poly((*S*)-(−)-MBZMI) obtained by AIBN (3) showed a similar peak to that with BuLi (2), but a different peak from that of poly((*R*)-(+)-MBZMI) obtained with AIBN under the same conditions, because the poly((*S*)-(−)-MBZMI) obtained with AIBN had lower M_n and polydisperse degree than that of poly((*R*)-(+)-MBZMI) with AIBN.

To clarify the dependence of temperature on specific rotation of optically active poly((*S*)-(−)-MBZMI) ($[\alpha]^{25}_{435}$ +551.7°, Run 4 in Table III) (1), ($[\alpha]^{25}_{435}$ +466.2°, Run 4 in Table III) (2) and ($[\alpha]^{25}_{435}$ +346.9°, Run 1 in Table III) (3), specific rotations were measured in $CHCl_3$ at several temperatures. Figure 8 shows the results of changes in specific rotations at various temperatures. The temperature coefficients ($|\Delta[\alpha] / \Delta T|$) of the polymers (1), (2), and (3) were 0.94, 0.65, and 0.33, respectively, and increased with specific rotation of the polymers. Polymers with higher specific rotation may thus contain much more of a helical structure.

Figure 9 shows X-Ray diffraction (XRD) diagrams for poly((*S*)-(−)-MBZMI)s obtained with Et_2Zn/Sp (1) Et_2Zn/Bnbox (2) *n*-BuLi (3) and AIBN (4). Width of XRD peaks is related to crystallinity degree.[26,27] A small crystallinity degree results in a broaden peak. A larger crys-

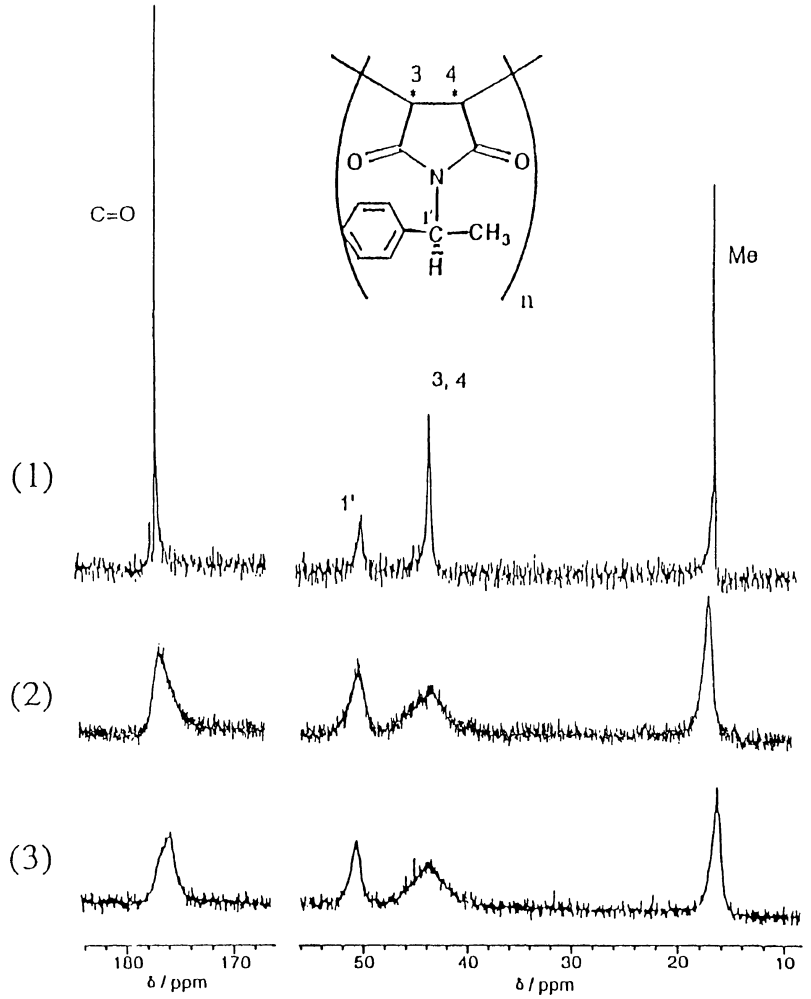

Figure 7. Expanded ^{13}C NMR spectra for poly((*S*)-(−)-MBZMI) obtained with (1) Et_2Zn/Sp (Run 4 in Table III), (2) *n*-BuLi (Run 1 in Table I), and (3) AIBN (Run 7 in Table I).

tallinity degree leads to a narrow peak.[25,26] From our results, crystallinity degrees of the polymers increased in proportion to specific rotations of the polymers, as shown in Figure 9. The higher the specific rotations of polymers, the greater was the crystallinity were, suggesting that polymers with higher specific rotation contain higher stereoregularity. Poly((*S*)-(−)-MBZMI) formed by Et_2Zn/Sp at −35℃ for 144 h had the most crystallinity (28.6%). The polymer may contain partially helical structures, due to threo-diisotactic configuration with occasional syndiotactic configuration which disrupts crystallinity. XRD curves of poly((*S*)-(−)-MBZMI)s obtained from Et_2Zn/Bnbox, *n*-BuLi, and AIBN showed no characteristic crystalline peaks, as shown in Figure 9, indicating that the polymers are not crystalline but complete amorphous. In these polymerizations, syndiotactic additions possibly took place, resulting in lower stereoregularity and specific rotations.

For poly((*S*)-(−)-MBZMI)s having higher specific rotations (Run 3 and Run 4 in Table III), THF-insoluble (a) and THF-soluble (b) parts exhibited crystalline peaks, as shown in Figure 10. The peak of THF-soluble part (b) of polymer showed a more disordered crystalline pattern than that of the THF-insoluble one (a). The crystallinity of the THF soluble part was relatively small. THF-insoluble parts had larger crystallinity, and XRD exhibited two stronger peaks at 4.5 Å and 8.0 Å. These results are consistent with those reported by Cubbon previously.[28] The poly(RMI) model made by Cubbon[28] indicated threo-diisotactic polymers to form the 3_1 helix with a repeat distance of 4.7 Å regardless of the substituent on nitrogen. But the diameter of helix vary with substituent on the nitrogen. Our result suggests that part of crystallinity in the polymer arose from helix produced by the threo-diisotactic configuration. Poly((*S*)-(−)-MBZMI) having higher dextro specific rotation may contain (*S, S*) more than (*R, R*) configuration, judging from results reported previously.[8] The poly((*S*)-(−)-MBZMI) had higher stereoregularity, compared with poly((*R*)-(+)-MBZMI).[17]

CONCLUSIONS

1. Asymmetric anionic polymerizations of chiral (*S*)-(−)-MBZMI were carried out with Et_2Zn/Sp and Et_2Zn/Bnbox to obtain optically active polymers. Poly((*S*)-(−)-MBZMI) obtained with Et_2Zn/Sp in toluene at −35℃ for 144 h showed the highest dextro specific rotation of +466.2°. Poly((*S*)-(−)-MBZMI) obtained with Et_2Zn/Bnbox at r.t. in THF showed the highest dextro specific

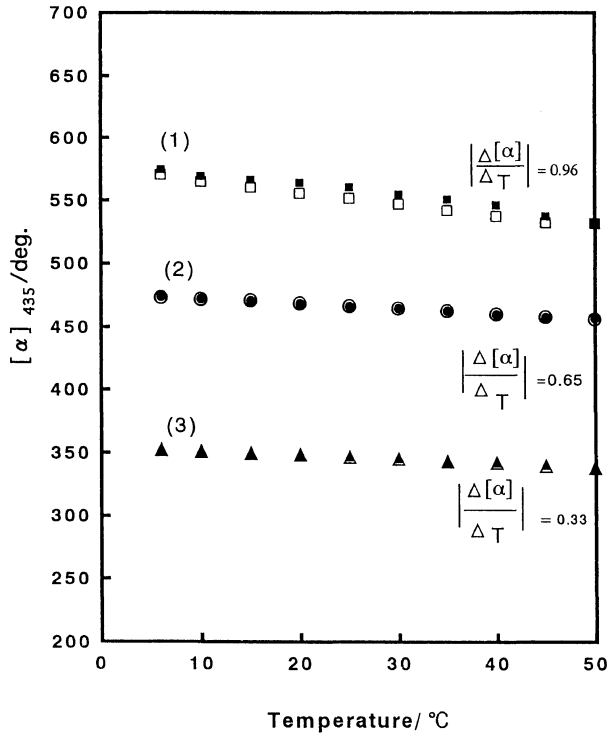

Figure 8. Effects of temperatures on $[\alpha]_{435}^{25}$ of poly((*S*)-(−)-MBZMI in solvent: $CHCl_3$, $c=1$ g dL^{-1}, $l=5$ cm. (1) ($[\alpha]_{435}^{25}$+ 571.2°): □ cooling, ■ heating, (2) ($[\alpha]_{435}^{25}$+466.2°): ○ cooling, ● heating, (3) ($[\alpha]_{435}^{25}$+346.9°): △ cooling, ▲ heating.

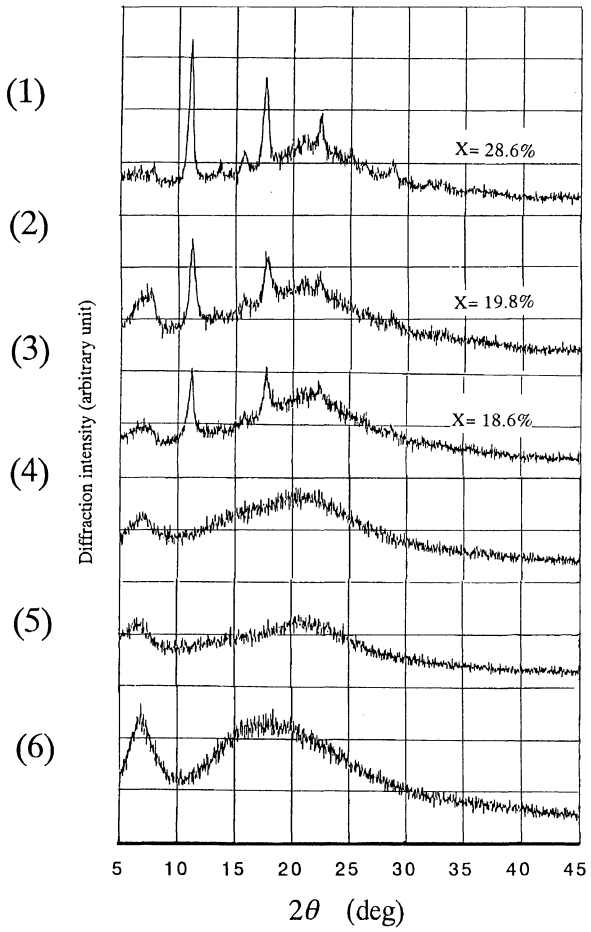

Figure 9. X-Ray diffraction diagrams for poly((*S*)-(−)-MBZMI) obtained with (1) Et_2Zn/Sp: $[\alpha]_{435}$ +466.2°, (2) Et_2Zn/Sp: $[\alpha]_{435}$ + 410.6°, (3) Et_2Zn/Sp: $[\alpha]_{435}$ +409.4°, (4) Bnbox: $[\alpha]_{435}$ +39.5°, (5) *n*-BuLi: $[\alpha]_{435}$ −7.8° and (6) AIBN: $[\alpha]_{435}$ −30.1°.

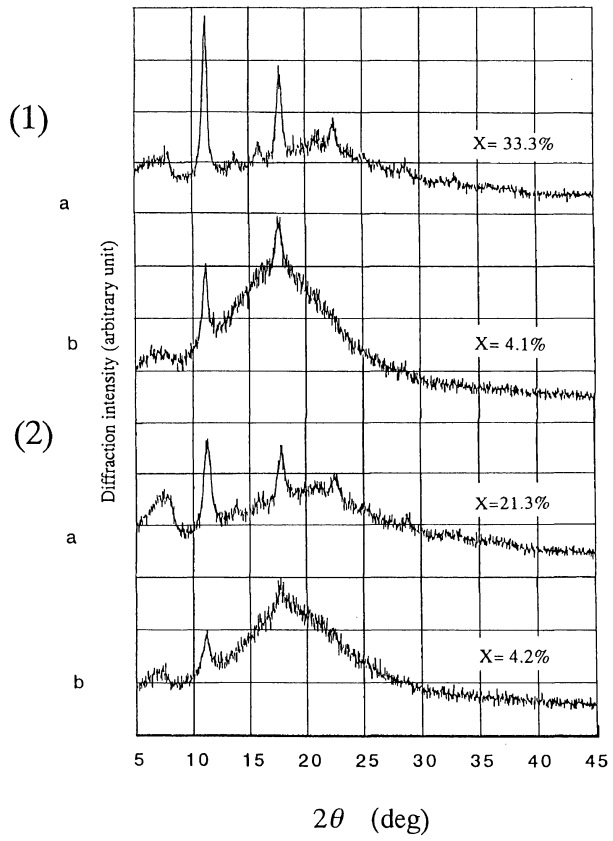

Figure 10. X-Ray diffraction diagrams for poly((*S*)-(−)-MBZMI) obtained with Et_2Zn/Sp: (1) a: $[\alpha]_{435}$ +551.7°, b: $[\alpha]_{435}$ +111.9° (Run 4 in Table III); and (2) a: $[\alpha]_{435}$ +488.4°, b: $[\alpha]_{435}$ +145.1° (Run 3 in Table III).

rotation of +39.5°.

2. Those polymers exhibited different specific rotations and CD patterns from that of model compounds (*S*)-(−)-MBZSI, suggesting that asymmetric induction take place in the main chain of the polymers. Chirality of poly-((*S*)-(−)-MBZMI) was attributed to new asymmetric carbons in the main chain induced by chiral ligands and original chiral carbons in the side chain.

3. The polymers obtained with Et_2Zn/Sp in toluene at lower temperatures had higher stereoregularity and larger crystallinity, judging from ^1H NMR, ^{13}C NMR, and XRD spectra of poly((*S*)-(−)-MBZMI)s. These may partially contain the helical conformation.

Acknowledgment. We are indebted to Dr. K. Sakai in Yamakawa Chemical Industry Co. Ltd. for supplying the optically active α-methylbenzylamine.

REFERENCES

1. Y. Okamoto and T. Nakano, *Chem. Rev.*, **94**, 349 (1994).
2. Y. Okamoto and E. Yashima, *Angew. Chem. Ing. Ed.*, **37**, 1020 (1999).
3. E. Yashima, K. Maeda, and Y. Okamoto, *Nature*, **399**, 6735 (1999).
4. T. Oishi, H. Yamasaki, and M. Fujimoto, *Polym. J.*, **23**, 795 (1991).
5. K. Onimura, H. Tsutsumi, and T. Oishi, *Polym. Bull.*, **39**, 437 (1997).
6. K. Onimura, H. Tsutsumi, and T. Oishi, *Macromolecules*, **31**,

5971 (1998).
7. K. Onimura, H. Tsutsumi, and T. Oishi, *Chem. Lett.*, **1998**, 791.
8. T. Oishi, K. Onimura, Y. Isobe, and H. Tsutsumi, *Chem. Lett.*, **1999**, 673.
9. T. Oishi, K. Onimura, K. Tanaka, W. Horimoto, and H. Tsutsumi, *J. Polym. Sci., Part A: Polym. Chem.*, **37**, 437 (1999).
10. T. Oishi, K. Onimura, Y. Isobe, H. Yanagihara, and H. Tsutsumi, *J. Polym. Sci., Part A: Polym. Chem.*, **38**, 310 (2000).
11. Y. Okamoto, T. Nakano, H. Kobayashi, and K. Hatada, *Polym. Bull.*, **25**, 5 (1991).
12. T. Oishi, K. Kagawa, and M. Fujimoto, *J. Polym. Sci., Part A: Polym. Chem.*, **33**, 1341 (1995).
13. K. Kagawa and T. Oishi, *Polym. J.*, **27**, 579 (1995).
14. T. Oishi, K. Kagawa, and H. Nagata, *Polymer*, **38**, 1461 (1997).
15. T. Oishi, H. Nagata, and H. Tsutsumi, *Polymer*, **39**, 4135 (1998).
16. K. Kagawa and T. Oishi, *Polym. J.*, **28**, 1 (1996).
17. H. Zhou, K. Onimura, H. Tsutsumi, and T. Oishi, *Polym. J.*, **32**, 552 (2000).
18. T. Oishi and M. Fujimoto, *J. Polym. Sci., Part A: Polym. Chem. Ed.*, **22**, 2789 (1984).
19. P. Y. Reddy, S. Kondo, T. Toru, and Y. Ueno, *J. Org. Chem.*, **62**, 2652 (1997).
20. J. A. Riddick, W. B. Bunger, and T. K. Sakano, "Organic Solvent", John Wiley & Sons, Inc., New York, N.Y., 1986.
21. S. E. Denmark, N. Nakajima, O. J.-C. Nicaise, A.-M. Faucher, and J. P. Edwards, *J. Org. Chem.*, **60**, 4884 (1995).
22. H. Yuki, K. Ohta, Y. Okamoto, and K. Hatada, *J. Polym. Sci., Polym. Lett. Ed.*, **15**, 589 (1977).
23. K. Ohta, Y. Okamoto, K. Hatada, and H. Yuki, *J. Polym. Sci., Polym. Chem. Ed.*, **17**, 2917 (1979).
24. Y. Okamoto, K. Ohta, and H. Yuki, *Mcromolecules*, **11**, 724 (1978).
25. Y. Okamoto, K. Ohta, and H. Yuki, *Chem. Lett.*, **1977**, 617.
26. M. Asai, M. Tsubio, T. Shimanouchi, and S. Mizushima, *J. Phys. Chem.*, **59**, 322 (1955).
27. C. X. Liang and K. Hirabayshi, *J. Appl. Polym. Sci.*, **45**, 1937 (1992).
28. R. C. P. Cubbon, *Polymer*, **6**, 419 (1965).